J Mater Sci (2011) 46:6277–6284
DOI 10.1007/s10853-011-5417-8

ABBASCHIAN FESTSCHRIFT

Interfacial interactions of biomaterials in water decontamination applications

Maryam Shafahi · Kambiz Vafai

Received: 20 November 2010 / Accepted: 22 February 2011 / Published online: 8 March 2011

Abstract Understanding the fundamental aspects of transport through biomaterials is a necessity for a vast range of bio-related studies. Biofilm formation on the surface of adsorptive media such as granular activated carbon (GAC) has been extensively used to remove organic materials, nitrogen species, heavy metals, and other contaminants in wastewater treatment. In this study, a multi-layer mass transfer system consisting of the reactor's bulk fluid, diffusion layer, biofilm, and GAC is modeled. In order to consider the equilibrium at the interface of biofilm and activated carbon, Freundlich adsorption method is applied. The interfacial interactions are taken into account in the biodegradation process. The results of model prediction are compared with the available experimental data and show a very good agreement. The effect of biofilm formation on the reactor porosity is considered through a porous media approach. Furthermore, the influence of variation in particle diameters on the removal efficiency is studied. It can be seen that porosity alteration as a result of biofilm formation within the carbon bed has a noticeable effect on the removal efficiency.

Introduction

Biofilm is a dominant form of existence for bacteria in most natural and synthetic environments. Depending on the application area, they can be useful or harmful. They are helpful in bioremediation, microbial enhanced oil recovery, and metal extraction. On the other hand, biofilms are damaging for water pipes, heat exchangers, submarines, and body organs [1, 2]. Granular activated carbon (GAC) has been used as an adsorbent medium to extract a wide range of materials from liquid solutions or gaseous mixtures. They are highly porous and their large interior surfaces make them favorite adsorptive filters. Biofilm formation on the surface of GAC substantially increases its treatment efficiency in different applications [3–8]. Understanding the details of biofilm mechanisms and characteristics will lead to a more precise knowledge of contaminants fate in many natural and synthetic environments.

Scott et al. [9] performed an experimental study on decontamination of streams containing heavy metals and organic chemicals by GAC covered with biofilm. They concluded that carbon by itself is not an efficient adsorbent for heavy metals but with the aid of biofilm and its EPS, rate and quantity of metal extraction substantially increases. Liang et al. [3] studied the adsorption and biodegradation of chemical compounds on biological activated carbon (BAC) utilizing a continuous column with different media such as GAC, seeded glass bead, and seeded GAC. They concluded that adsorption is the prevailing mechanism for removal of the contaminating compound and biodegradation is the main key to eradicate ozonation intermediates. Ravindran et al. [10] studied mathematical models incorporating adsorption and mass transfer, and developed biofilm degradation for performance prediction of bioactive carbon fixed-bed and fluidized-bed adsorbers in wastewater treatment. Sensitivity analysis was performed to evaluate the effects of adsorption equilibrium, mass transfer, biokinetic and biofilm parameters.

Yang and Al-Duri [11] studied adsorption equilibrium and kinetics of three reactive dyes from their single-component aqueous solutions onto activated carbon in a batch

M. Shafahi · K. Vafai (✉)
Department of Mechanical Engineering, University of California, Riverside, CA 92521, USA
e-mail: vafai@engr.ucr.edu

reactor. They found out a kinetic model which generated the best agreement with the three adsorption systems' experimental data. Chudyk and Snoeyink [12] studied bioregeneration of GAC under conditions of typical water treatment plant operations. Kim et al. [13] developed a mathematical model that describes the adsorption and biodegradation phenomena in fluidized-bed absorbers. They observed that the model is satisfactory for an ideal biodegradable compound and wastewaters consisting of a large range of substrates. Liang et al. [14] focused on differentiating the adsorption and biodegradation quantities of a biologically activated carbon column and on evaluating the effect of empty bed contact time on the performance of these two mechanisms simultaneously for the removal of dissolved organic matter from water. They observed that the empty bed contact time could influence the performance of adsorption and biodegradation. Chang and Rittmann [7] studied the effect of attaching surface on biofilm shear loss with two different types of granular activated carbons. They observed that the shear loss is a function of surface coverage by biofilm and that it notably changes when the carbon is completely covered.

The biofilm interaction with metals has been studied in a wide range of applications [9, 15–19]. Malik [15] reported the successful and economically efficient removal of heavy metals by bacterial biofilms. Multispecies biofilms have shown more efficacies for different pH ranges and high metal concentrations. The extracellular polymeric substance (EPS) of the biofilm entraps the dissolved metals. Puranik et al. [16] investigated the biosorption of lead and zinc and interpreted the experimental data with a mathematical model based on the equilibrium of metal sorption and mass transfer kinetics. Lameiras et al. [17] studied the biosorption of Cr(VI) in different configuration of GAC and zeolite columns. The absorber media were covered with Arthrobacter viscous biofilm. They investigated the interactions among metal ions and functional group in the biomass utilizing Fourier transform infrared spectroscopy (FTIR).

The objective of this work is to study the chemical substrate removal through a multilayer mass transfer system in a reactor consisting of GAC covered with biofilm. The presented model takes into account the fundamental mechanisms of transport in bulk fluid, diffusion layer, biofilm, and GAC. Combination of all these mechanisms along with accounting for the interfacial phenomena provides us with a model which is able to predict the efficiency of biosorption for water decontamination. The effect of biofilm formation on the porosity of the carbon bed is considered. Biofilm occupies the available empty spaces in the GAC bed which influences the contaminant removal efficiency as our results show. To the authors' best knowledge, the porosity changes in the GAC bed has not been considered in any of the previous studies in this field.

Materials and methods

The simple schematic of multilayer mass transfer system including bulk fluid, diffusion layer, biofilm, and carbon can be seen in Fig. 1.

Bulk fluid

It is assumed that the biosorption occurs in a completely mixed biofilm reactor. A mass balance for the reactor provides us with the following equations for phenol and bacteria concentrations in the bulk fluid [5].

$$\frac{dC_{bulk}}{dt} = \underbrace{\frac{Q}{V\varepsilon}(C_0 - C_{bulk})}_{\text{inflow-outflow}} - \underbrace{\frac{3W_c h_m (R_c + L_f)^2}{V\varepsilon\rho_c R_c^3}(C_{bulk} - C_s)}_{\text{attachmenttothebiofilm}} - \underbrace{\frac{kC_{bulk}}{K_s + C_{bulk}}X_{bulk}}_{\text{reactioninthebulkfluid}} \quad (1)$$

$$\frac{dX_{bulk}}{dt} = \underbrace{\left(\frac{YkC_{bulk}}{K_s + C_{bulk}} - b - \frac{Q}{V\varepsilon}\right)X_{bulk}}_{\text{reactionandeffluent}} + \underbrace{\frac{3W_c b_s}{V\varepsilon\rho_c R_c}L_f X_f}_{\text{detachmentfromthebiofilm}} \quad (2)$$

where C_{bulk} is phenol concentration in the bulk fluid (M_{ph}/L^3), Q is the volumetric flow rate of the feed solution (L^3/T), V reactor volume (L^3), ε porosity of the reactor, Y yield of biomass (M_x/M_{ph}), k maximum rate of substrate utilization ($M_{ph}/(M_xT)$), W_c weight of carbon in the reactor (M_c), h_m diffusion layer mass transfer coefficient (L/T), R_c carbon particle diameter (L), ρ_c density of the carbon particle (M_c/L^3), L_f biofilm thickness (L), K_s half-velocity concentration (M_{ph}/L^3), X_{bulk} bacterial concentration in the bulk fluid (M_x/L^3) and X_f bacterial concentration in the biofilm (M_x/L^3).

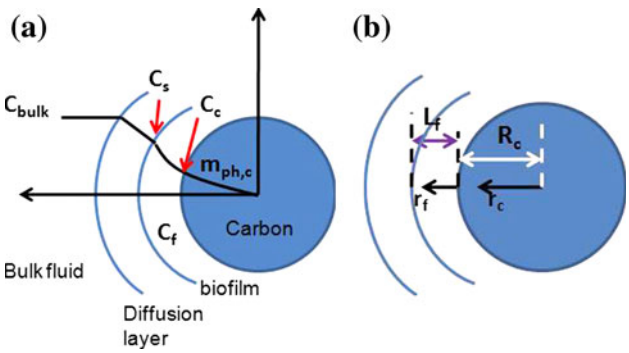

Fig. 1 **a** Schematic of the multilayer mass transfer system consisting of bulk fluid, diffusion layer, biofilm, and GAC; **b** coordinate systems for different layers

Biofilm phase

The biofilm model is based on the substrate diffusion and single Monod reaction [20] as can be seen below:

$$\frac{\partial C_f}{\partial t} = D_f \frac{\partial^2 C_f}{\partial r_f^2} - \frac{kC_f}{K_s + C_f} X_f \quad 0 \le r_f \le L_f \tag{3}$$

where C_f is the substrate concentration in biofilm (M_{ph}/L^3), D_f substrate diffusion coefficient in the biofilm (L^2/T), and r_f is the biofilm coordinate (L).

Biofilm boundary conditions

Substrate concentration at the surface of GAC is obtained from the Freundlich equilibrium as follows:

$$C_f|_{r_f=0} = C_c = \left(\frac{m_c}{K_c}\right)^n \tag{4}$$

where m_c is carbon adsorption capacity for phenol at the interface of biofilm and GAC (M_{ph}/M_c), and K_c is the Freundlich isotherm coefficient $\left(M_{ph}^{1-1/n} L^{-3/n}/M_c\right)$.

At the interface of biofilm and diffusion layer the mass flux continuity requires:

$$h_m(C_{bulk} - C_s) = D_f \left.\frac{\partial C_f}{\partial r_f}\right|_{r_f=L_f}; \quad C_s = C_f|_{r_f=L_f} \tag{5}$$

where h_m is the mass transfer coefficient in the diffusion layer taken form Williamson et al. [21] work based on the following correlation:

$$h_m = 2.40\, v_s \left(\frac{Re}{\varepsilon}\right)^{-0.66} (Sc)^{-.58} \tag{6}$$

where v_s is the superficial velocity in the reactor, ε porosity of the reactor, *Re* Reynolds number $\left(\frac{\rho(d_c+L_f)v_s}{\mu}\right)$; d_c is the carbon diameter; *Sc* is Schmidt number $\left(\frac{\mu}{\rho D}\right)$, and D is the diffusivity of water. It should be noted that due to variances in mass transfer relationships, other correlations are also considered in this work.

Biofilm growth

As the biofilm starts consuming the substrate, microorganisms continue their biosynthesis and respiration. Biofilm thickness variation versus time is a net effect of interactions among microbial growth, microbial decay, and shear stress as can be seen in the following equation:

$$\frac{d(L_f X_f)}{dt} = \int_0^{L_f} \left(\frac{YkC_f}{K_s + C_f} - b - b_s\right) X_f dr_f \tag{7}$$

$$L_f = L_0 \quad t = 0$$

where b is the biofilm decay coefficient (1/T) and b_s is biofilm shear loss coefficient (1/T).

Solid phase

The diffusion equation is used to account for the transport of substrate through the carbon particles assuming that no reaction occurs within the sphere.

$$\frac{\partial m_{ph,c}}{\partial t} = \frac{D_c}{r_c^2} \frac{\partial}{\partial r_c}\left(r_c^2 \frac{\partial m_{ph,c}}{\partial r_c}\right) \quad 0 \le r_c \le R_c \tag{8}$$

where $m_{ph,c}$ is the carbon adsorption capacity for phenol (M_{ph}/M_c), D_c substrate diffusion coefficient in the carbon (L^2/T), and r_c radial coordinate of the carbon particle (L), where M, L and T refer to mass, length, and time units, respectively.

The symmetry of the concentration profile within the sphere and Freundlich equilibrium at the carbon biofilm interface lead to the following boundary conditions:

$$m_{ph,c}\big|_{r_c=R_c} = K_c (C_c)^{1/n} \tag{9}$$

$$\left.\frac{\partial m_{ph,c}}{\partial r_c}\right|_{r_c=0} = 0 \tag{10}$$

where K_c is the Freundlich isotherm coefficient $\left(M_{ph}^{1-1/n} L^{-3/n}/M_c\right)$. Conservation of mass over GAC requires that the substrate mass entering the carbon particle has to be equal to the increase of mass storage inside the carbon particle. This results:

$$R_c^2 D_f \left.\frac{\partial C_f}{\partial r_f}\right|_{r_f=0} = \rho_c \frac{\partial}{\partial t} \int_0^{R_c} m_{ph,c} r_c^2 dr_c \tag{11}$$

Equations 1–11 take into account the fundamental substrate transport aspects through a multilayer system. This model considers the reaction and attachment in the bulk fluid, transport through the diffusion layer, diffusion and reaction in the biofilm, and diffusion within the spherical carbon particle. As mentioned before the reactor is assumed to be completely mixed and all the carbon particles are considered to have the same diameter.

Biofilm affected porosity

In order to study the effect of biofilm formation on the porosity of GAC bed, a cubic unit cell is chosen to represent the porous media and it is assumed that biofilm forms homogenously on the spherical surfaces.

The following relationship [1, 22] gives the biofilm affected porosity of the porous media represented by a cubic unit cell.

$$\varepsilon_b = 1 - \frac{V_b^s}{V} = 1 - \frac{\pi}{\alpha}\left(\frac{1}{6} + \frac{L_f}{d_c} + \left(2 - \frac{m}{2}\right)\left(\frac{L_f}{d_c}\right)^2 + \left(\frac{4}{3} - \frac{2m}{3}\right)\left(\frac{L_f}{d_c}\right)^3\right) \quad (12)$$

where α is the arrangement factor of the unit cell, d_c the carbon diameter, m the number of tangential contacts for each sphere with its neighbors within the unit cell and V_b^s is the volume occupied by carbon spheres and the biofilm formed over their surfaces. Figure 2a shows the unit cell that is utilized to represent the porous media network. It is assumed that biofilm homogenously covers the surface of spherical particles as can be seen in Fig. 2b.

Since the mass transfer coefficient is a function of the reactor porosity based on Eq. 6 as well as other mass transfer correlations (given in Eqs. 13 and 14), it changes with the biofilm formation inside the bed as well. We have utilized two other mass transfer correlations to show the effect of biofilm formation on removal efficiency. The following correlations were obtained from the works of Frantz [23] and Upadhyay and Tripathi [24], respectively.

Frantz (1962)

$$h_m = 5v_s\left(\frac{\mathrm{Re}}{1-\varepsilon}\right)^{-0.7}(Sc)^{-2/3} \quad (13)$$

Upadhyay and Tripathi (1975)

$$h_m = 3.8155v_s\left(\frac{\mathrm{Re}}{1-\varepsilon}\right)^{-0.7313}(Sc)^{-2/3} \quad (14)$$

The removal efficiency for the substrate is calculated from

$$\eta = 1 - \frac{C_{bulk}}{C_0} \quad (15)$$

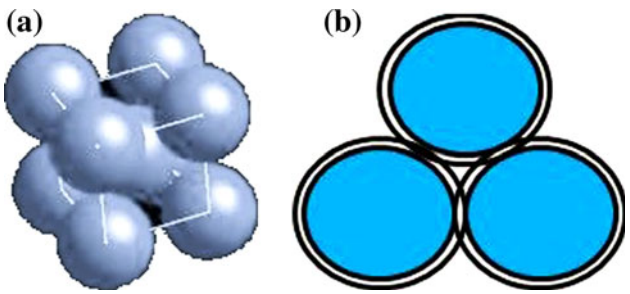

Fig. 2 **a** Cubic unit cell representation of the porous medium within the reactor, **b** cross-sectional area of cubic unit cell with biofilm coverage of the particles surfaces

Results and discussions

Phenol concentration in the bulk fluid obtained from the model calculations is compared with the experimental data given in Chang and Rittmann's [6] work, utilizing the physical parameters used in their model. As seen in Fig. 3, model predictions are in a very good agreement with the experimental data except an overestimation for the peak of the curve that occurs around 45 h after phenol injection into the feed solution. Figure 3 has the typical characteristics of an adsorptive carbon breakthrough curve, which displays almost negligible biofilm consumption before the peak. Biofilm growth catches up shortly after the maximum point and a substantial substrate concentration decrease occurs in the bulk fluid. Eventually, the substrate concentration reaches an almost constant level which can be considered as the final response of the treatment system.

The GAC is able to absorb the substrate from the biofilm and desorb into it. Figure 4 shows the profile of carbon adsorption capacity versus time at the center and the external surface of the particle. It can be seen that the adsorption turns to desorption sometime around the first day and finally carbon becomes saturated and $m_{ph,c}$ at the surface and center of the sphere become identical. In

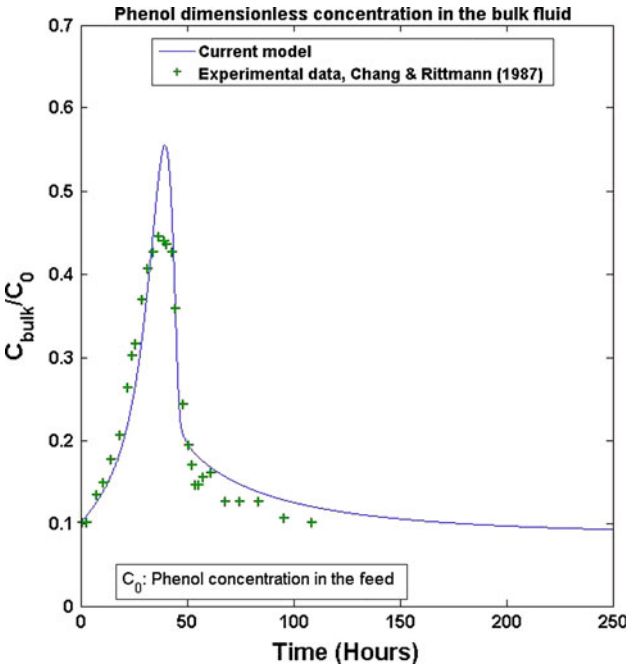

Fig. 3 Comparison of the model-based predicted data with experimental results of Chang and Rittmann [5] for phenol normalized concentration in the bulk fluid

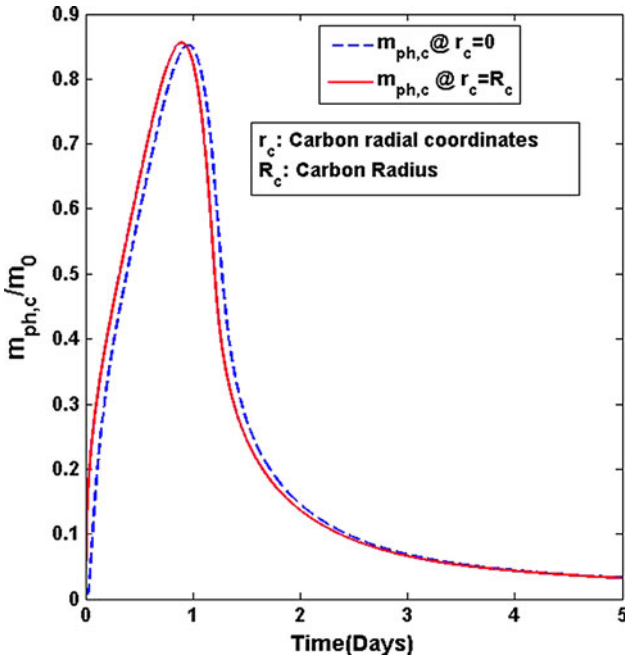

Fig. 4 Normalized carbon adsorption capacity at the center and the external surface of the sphere versus time

Fig. 5a and b, the spatial profile of adsorption capacity is shown after 1 and 4 days.

The formation of biofilm over the carbon particles leads to a reduction of the available empty spaces in the reactor which alters its porosity based on Eq. 12. As can be seen in Fig. 6, the mass transfer coefficient and removal efficiency change when accounting for the effect of biofilm formation on the reactor porosity. The diffusion layer mass transfer coefficient becomes smaller based on Eq. 6 (Williamson et al. correlation) and its magnitude will be affected by decreasing porosity due to the growth of biofilm thickness. Therefore, this causes an accelerated decreasing trend for the biofilm mass transfer coefficient, h_{mb} as seen in Fig. 6a. The removal efficiency of the system will be influenced by changes in mass transfer coefficient as shown in Fig. 6b.

The removal efficiency and mass transfer coefficient while considering and neglecting the effect of porosity alteration due to the biofilm formation is illustrated in Figs. 7 and 8 based on the other mass transfer correlation equations given in Eqs. 13 and 14. It can be seen that the porosity variation has a different influence on the mass transfer coefficient and removal efficiency of the system for these correlations. Since this method is used to a large extent in the water treatment, even a small miscalculation in the phenol content or other contaminants in the filtered water results in a substantial difference. Therefore, proper accounting of the porosity variation during the treatment process and its subsequent influence on the mass transfer through different layers is necessary to capture a more realistic picture of the described physical event.

Figure 9a and b displays the removal efficiency and mass transfer coefficient profiles for three different particle diameters based on Williamson et al. and Upadhyay and Tripathi correlations. These figures show the effect of carbon particle size on mass transfer coefficient ratio and removal efficiency of the system. The minimum change in the mass transfer coefficient occurs for the smallest carbon particles regardless of whether Williamson et al. or

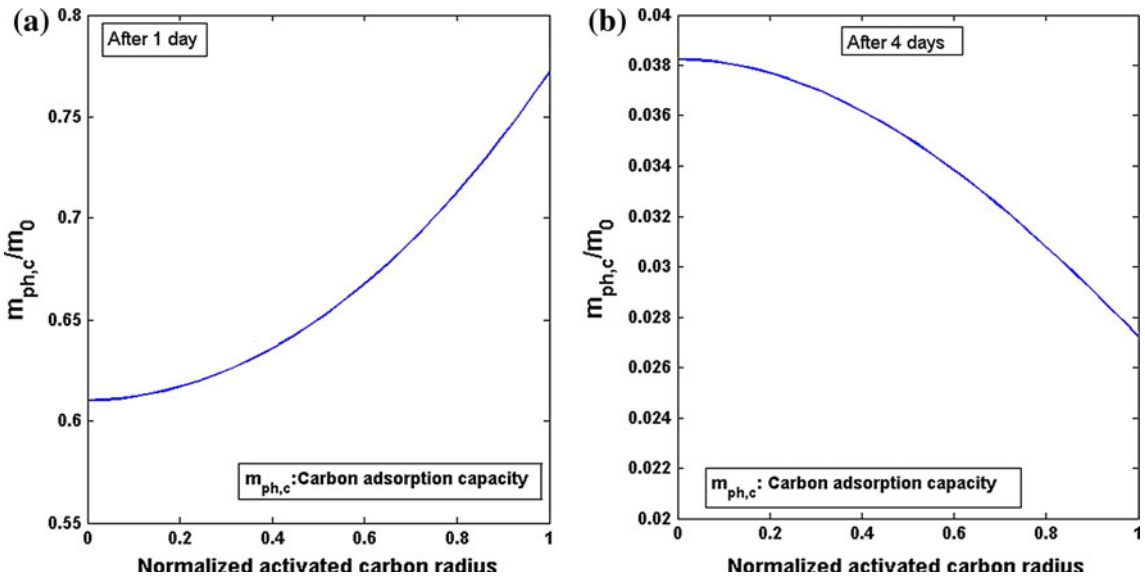

Fig. 5 Carbon adsorption capacity spatial profile **a** after 1 day; **b** after 4 days

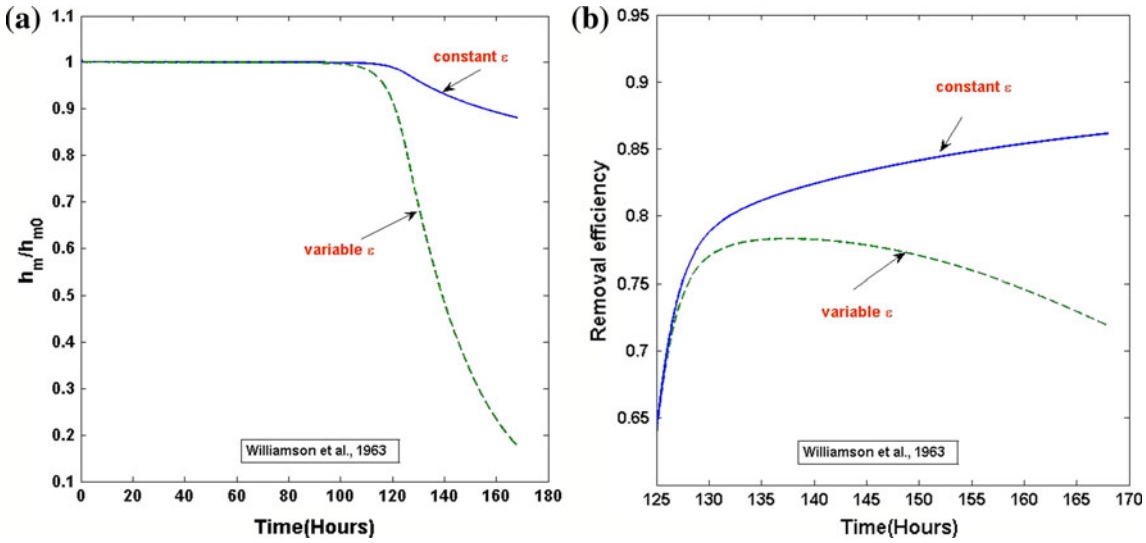

Fig. 6 Normalized profile of diffusion layer mass transfer coefficient and removal efficiency with and without the effect of change in the reactor porosity (Williamson et al. correlation)

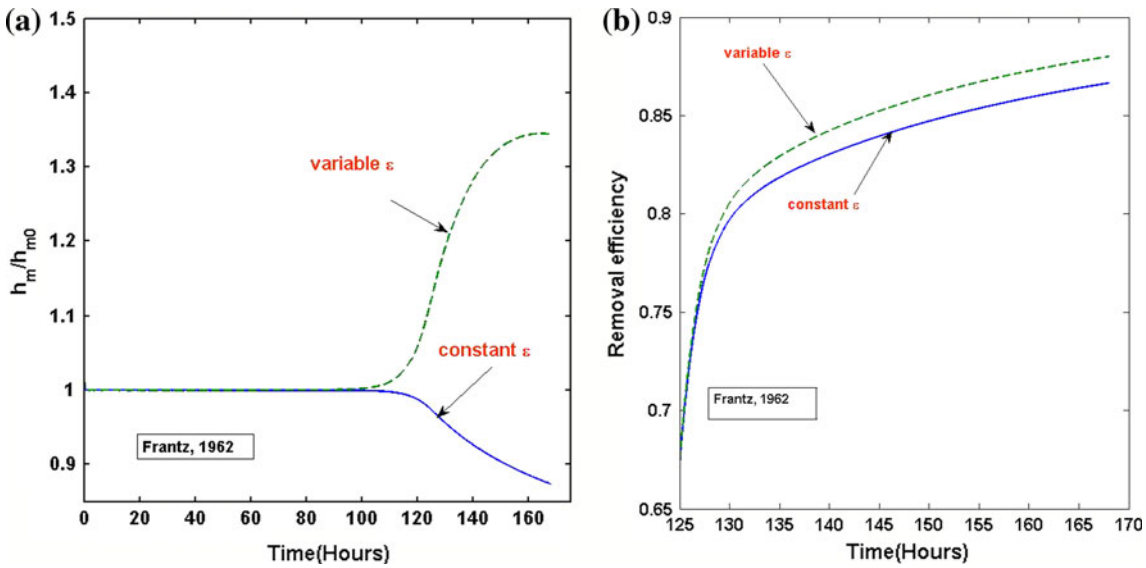

Fig. 7 Normalized profile of diffusion layer mass transfer coefficient and removal efficiency with and without the effect of change in the reactor porosity (Frantz correlation)

Upadhyay and Tripathi correlations are utilized as seen in Fig. 9b. Removal efficiency, which is affected by the biofilm growth is shown in Fig. 9a. As can be seen in Fig. 9a, the highest removal efficiency corresponds to the smallest size particles. This falls in line with the physical expectations. As can be seen in Eq. 1, the attachment term becomes larger when the particle diameter becomes smaller. This is due to enhancement of available contact surface for the case of small particles in the reactor. The sharp increase in the removal efficiency after approximately the first 100 h is related to the biofilm growth domination. Finally, biofilm thickness growth for different GAC sizes can be seen in Fig. 10, which also shows the least growth for the smallest size particles. This will in turn result in smaller porosity variations for the smaller size particles.

Conclusions

A comprehensive model was utilized to study the contaminant removal within a bed of GCA in a mixed reactor. The presented model accounted for the phenol removal

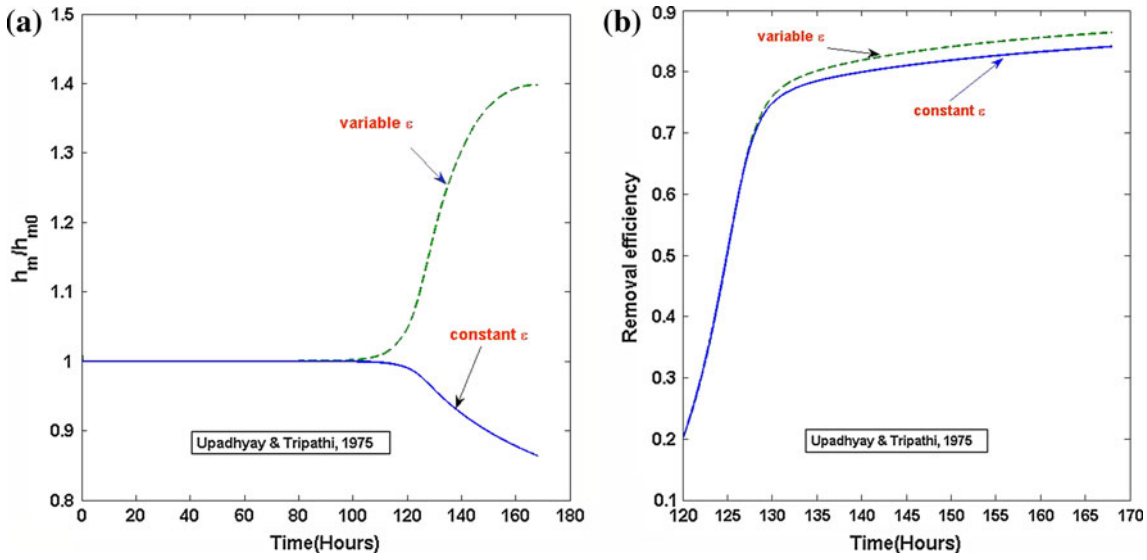

Fig. 8 Normalized profile of diffusion layer mass transfer coefficient and removal efficiency with and without the effect of change in the reactor porosity (Upadhyay and Tripathi correlation)

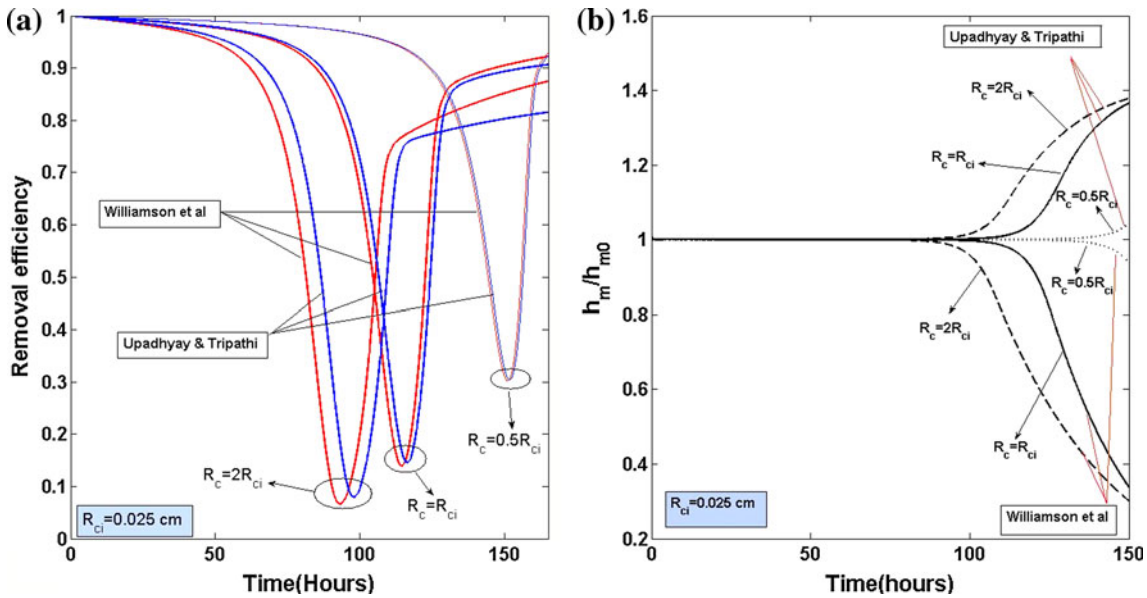

Fig. 9 **a** Removal efficiency of the reactor for different GAC diameters; **b** normalized diffusion layer mass transfer coefficient for different GAC diameters (based on Williamson et al. and Upudhyay and Tripathi correlations)

from the contaminated water. The fundamental aspects of mass transport through a multilayer system including the bulk fluid, diffusion layer, biofilm, and the carbon particle along with the interfacial interactions among the layers is taken into account. The model predictions displayed a very good agreement when compared with the available experimental data in literature. The effect of reactor porosity alteration due to the formation of biofilm on the carbon particles was accounted for by utilizing a porous media approach. Previous studies in this field [3–8] took the reactor porosity constant during the biosorption process. The mass transfer coefficient in the diffusion layer is influenced by the porosity variation in the bed and the removal efficiency becomes affected as a result of less available empty space in the reactor. Since this method of treatment is utilized extensively for drinking water, a small change in the concentration of the chemical compound in the solution makes a noticeable difference. The effect of

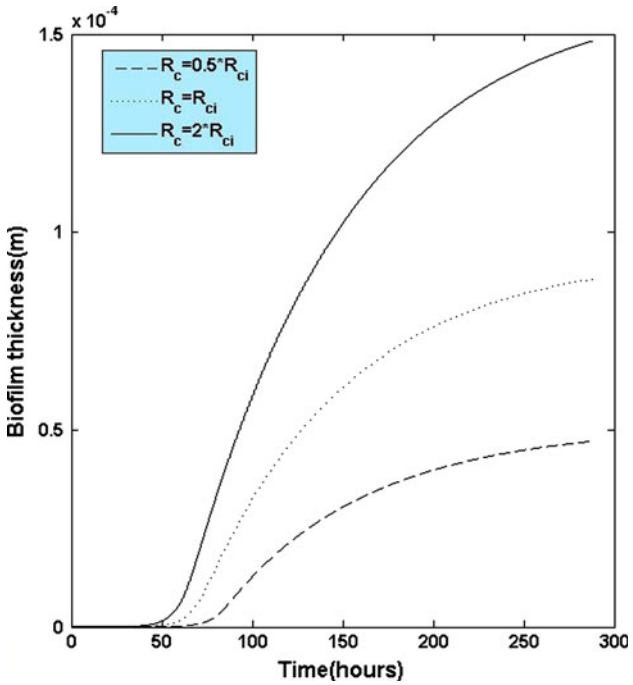

Fig. 10 Biofilm thickness profiles on the surface of carbon particles for different GAC diameters

porosity variation on the mass transfer coefficient is contradictory when utilizing different correlations from the literature. There is a need for clarification of the available correlations so as to obtain more precise modeling prediction in biosorption.

Finally, the effect of carbon particle diameter on the removal efficiency was also studied. It was established that reducing the particle size increases the removal efficiency of the reactor.

References

1. Shafahi M, Vafai K (2009) Int J Heat Mass Transf 52:574
2. Shafahi M, Vafai K (2010) Int J Heat Mass Transf 53:2943
3. Liang CH, Chiang PC, Chang EE (2003) Ozone Sci Eng 25:351
4. Liang CH, Chiang PC, Chang EE (2007) Water Res 41:3241
5. Chang HT, Rittmann BE (1987) Environ Sci Technol 21:273
6. Chang HT, Rittmann BE (1987) Environ Sci Technol 21:280
7. Chang HT, Rittmann BE (1988) Water Pollut Control Fed 60:362
8. Badriyha BN, Ravindrann V, Den W, Pirbazari M (2003) Water Res 37:4051
9. Scott JA, Karanjkar AM, Rowe DL (1995) Miner Eng 8:221
10. Ravindran V, Badriyha BN, Pirbazari M, Kim S-H (1996) Appl Math Comput 76:99
11. Yang X, Al-Duri B (2005) J Colloids Interface Sci 287:25
12. Chudyk WA, Snoeynik VL (1984) Environ Sci Technol 18:1
13. Kim S-H, Pirbazari M (1989) J Environ Eng 115:1235
14. Liang CH, Chiang PC, Chang EE (2004) J Chin Inst Chem Eng 35:203
15. Malik A (2004) Environ Int 30:261
16. Puranik PR, Modak JM, Paknikar KM (1999) Hydrometallurgy 52:189
17. Lameiras S, Quintelas C, Tavares T (2008) Bioresour Technol 99:801
18. Ferris FG, Schultze S, Witten TC, Fyfe WS, Beveridge TJ (1989) Appl Environ Microbiol 55:1249
19. Teitzel GM, Parsek MR (2003) Appl Environ Microbiol 69:2313
20. Rittmann BE, McCarty PL (1981) J Environ Eng Div 107:831
21. Williamson JE, Bazaire KE, Geankoplis CJ (1963) J Ind Eng Chem Fundam 2:126
22. Taylor SW, Milly PCD, Jaffe P (1990) Water Resour Res 26:2161
23. Frantz J (1962) Chem Eng 69:161
24. Upadhyay SN, Tripathi G (1975) J Chem Eng Data 20:20